



ELSEVIER

Physica E 4 (1999) 119–127

PHYSICA E

Resonantly enhanced bound–continuum intersubband second harmonic generation in optimized asymmetric semiconductor quantum wells

D. Indjin^{a,*}, A. Mirčetić^a, Z. Ikonić^a, V. Milanović^a, G. Todorović^b

^a*Faculty of Electrical Engineering, University of Belgrade, Bulevar Revolucije 73, 11120 Belgrade, Minor Yugoslavia*

^b*Faculty of Civil Engineering, University of Belgrade, Bulevar Revolucije 73, 11120 Belgrade, Minor Yugoslavia*

Received 17 July 1998; accepted 9 November 1998

Abstract

A systematic procedure applied to a step-asymmetric quantum well in order to maximize intersubband bound–continuum second-order susceptibility is described. The possibility is explored of obtaining resonantly enhanced nonlinear optical susceptibilities in quantum wells with two bound and a continuum resonance state as the dominant third state. This would significantly extend the range of input radiation photon energies that may be frequency doubled under resonance conditions in realistic structures. Calculation for the $\text{Al}_x\text{Ga}_{1-x}\text{As}$ alloy based wells designed for pump photon energies in range of $\hbar\omega = 200\text{--}300\text{ meV}$ indicate a perspective of employing continuum states in resonant second harmonic generation at higher photon energies. © 1999 Elsevier Science B.V. All rights reserved.

PACS: 73.20Dx

Keywords: Nanostructures; Quantum wells; Optical properties

1. Introduction

Recently, band gap engineering of semiconductor quantum well (QW) structures has been employed for optimizing the performance of various QW-based devices [1]. In particular, there has been an increasing interest in nonlinear optical effects based on intersubband transitions between quantized states in QWs [2–17]. This is related to large values of transition matrix

elements between these states, and to the fact that the quantized states energies and wave functions in QWs are continuously “tailorable” in a rather broad range (corresponding to mid-infrared radiation), making it possible to design QWs with resonantly enhanced nonlinearity for a particular wavelength. Among various nonlinear processes, most attention has been paid to the resonant second harmonic generation (SHG), which requires an asymmetric QW structure. To be resonantly enhanced, this process requires three states spaced by the “pump” photon energy. It has been customary to take all three states to be bound, and various

* Corresponding author. E-mail: indjin@kiklop.etf.bg.ac.yu.

asymmetric QWs were analyzed for this case, e.g. compositionally graded, in a stepwise-constant manner, step QWs [3–7], electric field biased QWs [8,9], and asymmetric coupled QWs [10–12]. Recently, some research effort has been put into finding the best potential shape of continuously graded QWs [13–16].

Most of the papers published so far describe resonant SHG for $\hbar\omega = 116$ meV which corresponds to CO₂ laser input [3–16] or even larger wavelengths [17]. The principal reason for this is that high power sources of this type are readily available and that it is rather straightforward to achieve conditions necessary for SHG in common GaAs/Al_xGa_{1-x}As-based QWs. When increasing the pump photon energies significantly above 116 meV, it becomes increasingly difficult or impossible to design a suitable QW, because it has to accommodate three bound states while the maximum height of the barrier (the conduction band offset) is limited in real semiconductors-QW constituents. Higher values of $\hbar\omega$ may be accessed by using bound-to-continuum transitions. States above the barrier, close to transmission resonances, may be favorable as the third state. The bound-continuum intersubband transitions have previously been considered in other contexts, e.g. for infrared absorption and photodetectors [18–23], but not for the harmonic generation.

In this paper we explore the possibility of using QWs with two bound states and above the barrier resonant continuum state for higher-energy intersubband SHG. The method of optimizing the QWs potential shape (in respect to the second-order susceptibility), handling step asymmetric QWs, relies on finding the solution to a system of nonlinear equations containing a few free parameters. The described procedure is systematic in the sense that all potentials of given class are explored, i.e. no potential better than that found as optimal may exist in that class. Calculations were performed for GaAs/Al_xGa_{1-x}As-based QWs which, introducing bound-to-continuum transitions, enable higher energy ($\hbar\omega = 200$ – 300 meV) intersubband resonant SHG.

2. Theoretical considerations

In *n*-doped QWs based on direct band gap semiconductor (with band gap large enough that inter-

band transitions may be neglected) the polarization response of the structure to the pump field with photon energy $\hbar\omega$ is mainly governed by intersubband transitions between quantized (bound or continuum) conduction band states E_i . Nonlinear polarization at twice the frequency of the pump field, acting as the source of second harmonic field is described by the second-order susceptibility $\chi^{(2)}$. Under the conditions stated above $\chi^{(2)}$ is significant only for both the pump and harmonic polarized perpendicular to the QW plane (*z*-axis), i.e. $\chi^{(2)} \equiv \chi_{zzz}^{(2)}$. It is given by the general expression (e.g. Ref. [5]):

$$\chi_{zzz}^{(2)} = \frac{e^3}{L_z \epsilon_0} \sum_i \sum_j \frac{1}{(2\hbar\omega - \Delta E_{ji}) - i\hbar\Gamma_{ji}} \times \sum_l M_{ij} M_{jl} M_{li} \times \left[\frac{\rho_{ii} - \rho_{ll}}{\hbar\omega + \Delta E_{li} - i\hbar\Gamma_{li}} - \frac{\rho_{ll} - \rho_{jj}}{\hbar\omega - \Delta E_{jl} - i\hbar\Gamma_{jl}} \right], \quad (1)$$

where $M_{ij} = \langle \Psi_i | z | \Psi_j \rangle$ are the transition dipole matrix elements, ΔE_{ij} the transition energies between states *i* and *j*, ρ_{ii} denotes the electron sheet density corresponding to state *i*, Γ_{ij} the off-diagonal relaxation rates and L_z the length of the structure. It is worth noting that the summation over 2D in-plane wave vector states is already performed in Eq. (1), so sheet densities ρ_{ii} appear therein. In majority of feasible structures almost all electrons normally reside on the lowest state (i.e. $\rho_{ii} \ll \rho_{00}$ for $i > 0$). In case of having continuum (free) states contributing the process, we consider the asymmetric QW with two bound states (with energies E_0 and E_1) and continuum states E_{cont} ($E_{\text{cont}} > U_B$). Energy of continuum states is described by the perpendicular (to the QW plane) wave vector k_B in the barrier region, i.e. $E_{\text{cont}}(k_B) = \hbar^2 k_B^2 / 2m_B$, where m_B is the effective mass in the barrier. Continuum states will hereafter be labeled with k_B subscript. Because of the denominators with energy differences, the expression for $\chi_{zzz}^{(2)}$ grossly simplifies under resonance conditions, i.e. when some of the states are spaced by about the “pump” photon energy $\hbar\omega$, with just one term with these “properly spaced” states remaining as important (resonantly enhanced). Taking that only the ground state is significantly populated with electrons, and the QW is tailored so that the two bound states are spaced by exactly the pump photon

energy $E_1 - E_0 = \Delta E_{01} = \hbar\omega$, $\chi_{zzz}^{(2)}$ is then found to be

$$\chi_{zzz}^{(2)} = \frac{e^3}{L_z \varepsilon_0} \frac{\rho_{00}}{i\hbar\Gamma_{01}} M_{01} \times \sum_{k_B} \frac{M_{0k_B} M_{1k_B}}{2\hbar\omega - [(E_{k_B} - E_0)] - i\hbar\Gamma_{0k_B}}. \quad (2)$$

The summation in Eq. (2) is performed over all continuum states. Wave functions corresponding to the states above the barrier are normalized by using the box-boundary conditions. The real part of $\chi_{zzz}^{(2)}$, which is of our interest, may then be written as

$$\chi_{zzz}^{(2)} = \frac{e^3}{L_z \varepsilon_0} \rho_{00} M_{01} \frac{1}{L_z} \sum_{k_B} \frac{\hat{M}_{0k_B} \hat{M}_{1k_B}}{(\hbar\Gamma)^2 + [(2\hbar\omega) - (E_{k_B} - E_0)]^2} \frac{\Delta k_B}{\Delta k_B}. \quad (3)$$

Certainly, the summation over the other two wave vector components of essentially 3D continuum states was already performed in Eq. (1). Furthermore, M_{01} is the bound-bound matrix element, \hat{M}_{0k_B} and \hat{M}_{1k_B} represent matrix elements calculated with normalized bound state (0 or 1) and nonnormalized above the barrier state real wave functions. We here take $\Gamma_{01} = \Gamma_{0k_B} = \Gamma_{1k_B} = \Gamma$ (line width $\hbar\Gamma$ is here taken to be common to all transitions), as is often assumed for bound states in the literature. In fact, this is not quite true, the electron scattering-induced part of the line width may be significantly different, but within the order of magnitude, for various transitions. However, the transitions-to-continuum states have another component of the line width, stemming from the width of the resonance, and it almost always dominates other sources of broadening. In particular, for the QWs treated in this work we find the resonance widths ≥ 30 meV, while we used the value $\hbar\Gamma = 5$ meV, so it is clear that doubling or even tripling this latter value would not change the final results too much. The matrix elements with states belonging to the continuum are to be calculated twice, because of the double degeneracy (i.e. with both wave functions corresponding to energy E_{k_B}). These two wave functions should be taken in the form of scattering states (i.e. to be orthogonal), which prevents under or over completeness in summing over all continuum states in Eq. (3). In the full continuum limit: $L_z \rightarrow +\infty$, $\Delta k_B \rightarrow dk_B$

and $\sum \rightarrow \int$, and with $\Delta k_B = \pi/L_z$ Eq. (3) becomes

$$\chi_{zzz}^{(2)} = \frac{e^3 \rho_{00}}{L_z \varepsilon_0} \frac{M_{01}}{\pi} \times \int_{(k_B)} \frac{\hat{M}_{0k_B}(E_0, E_{k_B}) \hat{M}_{1k_B}(E_1, E_{k_B})}{(\hbar\Gamma)^2 + [(2\hbar\omega) - (E_{k_B} - E_0)]^2} dk_B \equiv \frac{e^3}{L_z \varepsilon_0} \rho_{00} \Pi^*. \quad (4)$$

In QWs with two bound states wave functions localized in the well, one expects that the continuum states wave functions close to the resonances (i.e. $E_{k_B} = E_{\text{res}}$) will give the largest contribution in Eq. (4), because of the largest matrix elements \hat{M}_{0k_B} and \hat{M}_{1k_B} (the continuum wave function amplitudes inside the well are larger at resonance energies than off them, but there is no difference outside the well, due to the normalization condition). The contribution of resonance states is particularly enhanced at photon energies for which $E_{k_B} - E_0 \approx 2\hbar\omega$, as follows from the denominator of Eq. (4). For these two reasons, the largest $\chi^{(2)}$ is to be expected with double resonance achieved with the two bound and a resonance state, i.e. $E_{k_B} - E_0 = E_{\text{res}} - E_0 = 2(E_1 - E_0) = 2\hbar\omega$.

In order to optimize the QW shape in respect to the second-order susceptibility, one may vary the shape (and hence the wave functions) subject to the constraint that the spacings between the relevant states remain unchanged, and look for the value of susceptibility (i.e. parameter Π^*), which still depends on the QW shape (via the dipole matrix elements). In case of $\chi^{(2)}$, because of definite parity of wave functions, symmetric QWs are ruled out, so one should consider asymmetric structures only.

Quantized electron states in a QW structure with position-dependent effective mass $m(z)$ may be found by solving the envelope function Schrödinger equation of the form [24]

$$-\frac{\hbar^2}{2} \frac{d}{dz} \left(\frac{1}{m(z)} \frac{d\Psi}{dz} \right) + U(z)\Psi = E\Psi, \quad (5)$$

where $\Psi(z)$ is envelope wave function, $U(z)$ the potential and E the energy. Effects of bulk dispersion nonparabolicity become increasingly important at higher energies and may be conveniently described by

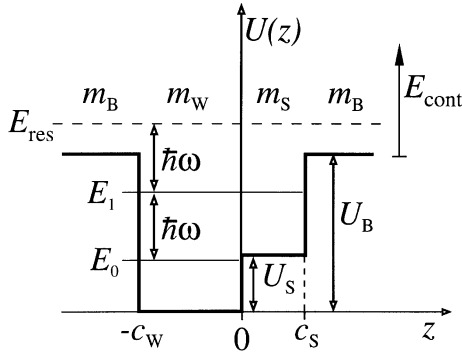


Fig. 1. The potential (conduction band edge) in step QW in case of two bound and one resonant state. The structure design parameters, used in the main text, are all denoted.

energy-dependent effective mass, according to the two-band Kane model [25]

$$m(z, E) = m^*(z) \left[1 + \frac{E - U(z)}{E_g(z)} \right], \quad (6)$$

where $E_g(z)$ is the material composition- (and hence the position-) dependent band gap, and $m^*(z)$ denotes the parabolic (band edge) effective mass.

Consider an asymmetric step QW with stepwise-constant potential and effective mass (Fig. 1), which is frequently used in bound-bound transitions-based resonant SHG. States above the barrier ($E > U_B$) are double degenerate, and their wave functions may be written in terms of scattering states:

$$\begin{aligned} \Psi_L(z) &= e^{ik_B z} + R_L e^{-ik_B z}, \quad z < -c_W, \\ \Psi_L(z) &= A_L e^{ik_W z} + B_L e^{-ik_W z}, \quad z \in (-c_W, 0), \\ \Psi_L(z) &= C_L e^{ik_S z} + D_L e^{-ik_S z}, \quad z \in (0, c_S), \end{aligned} \quad (7)$$

$$\begin{aligned} \Psi_L(z) &= T_L e^{ik_B z}, \quad z > c_S, \\ \Psi_R(z) &= T_R e^{-ik_B z}, \quad z < -c_W, \\ \Psi_R(z) &= A_R e^{ik_W z} + B_R e^{-ik_W z}, \quad z \in (-c_W, 0), \\ \Psi_R(z) &= C_R e^{ik_S z} + D_R e^{-ik_S z}, \quad z \in (0, c_S), \end{aligned} \quad (8)$$

$$\Psi_R(z) = e^{-ik_B z} + R_R e^{ik_B z}, \quad z > c_S,$$

where $k_B = [2m_B(E - U_B)/\hbar^2]^{1/2}$, $k_W = [2m_W E/\hbar^2]^{1/2}$, and $k_S = [2m_S(E - U_S)/\hbar^2]^{1/2}$ are the wave vectors in the barrier, deeper well and the step layers with the corresponding energy-dependent nonparabolic effective masses $m_B(E)$, $m_W(E)$ and

$m_S(E)$. The constants in Eqs. (7) and (8) should be determined by using the conventional boundary conditions (the continuity of $\Psi(z)$ and $(1/m(z))d\Psi/dz$) at heterointerfaces ($z = -c_W, 0$ and c_S). As we have pointed above, the most interesting states above the barrier are those close to resonances. Energies of resonances are found from the transmission coefficient which in this structure reads

$$|T_R|^2 = |T_L|^2 = \frac{4\eta^2 \zeta^2}{|\xi|^2}, \quad (9)$$

where $\eta = (m_S k_B)/(m_B k_S)$, $\zeta = (m_S k_W)/(m_W k_S)$ and

$$\begin{aligned} |\xi|^2 &= \eta^2(1 + \zeta^2) \sin^2(k_W c_W) \sin^2(k_S c_S) \\ &+ 4\eta^2 \zeta^2 \cos^2(k_W c_W) \cos^2(k_S c_S) \\ &+ 2\zeta(\eta^2 - \zeta^2)(\eta^2 - 1) \sin(k_W c_W) \\ &\times \sin(k_S c_S) \cos(k_W c_W) \cos(k_S c_S) \\ &+ (\eta^2 + \zeta^2) \sin^2(k_W c_W) \cos^2(k_S c_S) \\ &+ \zeta^2(1 + \eta^2) \cos^2(k_W c_W) \sin^2(k_S c_S). \end{aligned} \quad (10)$$

Resonances correspond to local maxima of transmission, which generally do not exactly equal unity in asymmetric systems [26–28]. After some manipulation, one finds that the positions of the transmission coefficient maxima coincide with minima of the following function:

$$\begin{aligned} F(E) &= A \sin^2(k_W c_W) \sin^2(k_S c_S) \\ &+ B \sin^2(k_W c_W) \cos^2(k_S c_S) \\ &+ C \cos^2(k_W c_W) \sin^2(k_S c_S) \\ &+ \frac{1}{2} D \sin(2k_W c_W) \sin(2k_S c_S) \\ &+ 2 \sin^2(k_W c_W) \sin^2(k_S c_S) - 2 \sin^2(k_W c_W) \\ &- 2 \sin^2(k_S c_S), \end{aligned} \quad (11)$$

where $A = (m_W k_S/m_S k_W)^2 + (m_S k_W/m_W k_S)^2$, $B = (m_W k_B/m_B k_W)^2 + (m_B k_W/m_W k_B)^2$, $C = (m_S k_B/m_B k_S)^2 + (m_B k_S/m_S k_B)^2$, $D = (m_B^2 k_W k_S/m_W m_S k_B^2 + m_W m_S k_B^2/m_B^2 k_W k_S - m_W k_S/m_S k_W - m_S k_W/m_W k_S)$. This defines the function $F(E)$, minima of which give us the continuum resonance energies E_{res} in the asymmetric step QW given in Fig. 1.

For convenience, instead of the complex wave functions of free states, Eqs. (7) and (8), we choose to make their linear combinations (unitary transforms) as

$$\Psi_1(z) = \frac{1}{\sqrt{2}} \left[\sqrt{\frac{R_R}{R_L}} \psi_L(z) + \psi_R(z) \right], \quad (12)$$

$$\Psi_2(z) = \frac{1}{\sqrt{2}} \left[-\sqrt{\frac{R_R}{R_L}} \psi_L(z) + \psi_R(z) \right] \quad (13)$$

which are entirely real functions (as also are the bound states wave functions), as shown in the appendix.

Below the barrier the (nondegenerate) bound states are found in the usual way, observing the boundary conditions at $z = -c_W, 0$ and c_S . With the conventional exponential or plane wave type of solutions of Eq. (5) in separate layers of the structure (Fig. 1) we get a system of six homogeneous equations, nontrivial solution of which requires that

$$\begin{aligned} \Phi(E) = \sin(k_W c_W) & \left[\sin(k_S c_S) \frac{k_B^*}{m_B} \left(\frac{k_W^2}{m_W^2} + \frac{k_S^2}{m_S^2} \right) \right. \\ & + \cos(k_S c_S) \frac{k_S}{m_S} \left(\frac{k_W^2}{m_W^2} - \frac{k_B^{*2}}{m_B^2} \right) \\ & - \cos(k_W c_W) \frac{k_W}{m_W} \left[\sin(k_S c_S) \left(\frac{k_B^{*2}}{m_B^2} - \frac{k_S^2}{m_S^2} \right) \right. \\ & \left. \left. + 2 \cos(k_S c_S) \frac{k_B^* k_S}{m_B m_S} \right] \right] = 0 \end{aligned} \quad (14)$$

in the energy range ($U_S < E < U_B$), where $k_B^* = ik_B = [2m_B(U_B - E)/\hbar^2]^{1/2}$. In energy range below the step ($0 < E < U_S$) we define $k_S^* = ik_S = [2m_S(U_S - E)/\hbar^2]^{1/2}$ and Eq. (7) is modified by substituting $\sin(k_S c_S) \rightarrow \sinh(k_S^* c_S)$, $\cos(k_S c_S) \rightarrow \cosh(k_S^* c_S)$, $k_S \rightarrow k_S^*$, $k_S^2 \rightarrow -k_S^{*2}$. This defines the function $\Phi(E)$, zeros of which are the energies of quantized bound states in asymmetric step QW. The corresponding bound states wave functions are then simply derived from the boundary conditions and the normalization condition $\int_{-\infty}^{+\infty} |\Psi(z)|^2 dz = 1$.

Having chosen the alloy system to work with (e.g. $\text{Al}_x\text{Ga}_{1-x}\text{As}$) it is reasonable to take the well layer to comprise pure “well-type” semiconductor (GaAs in this instance), because, with dipole matrix elements roughly scaling as effective mass to power $\frac{1}{2}$ [5] there is no benefit from allowing the well layer to be made

of alloy. Thus, m_W is defined from the start, and in the step and barriers layers, which are made of the alloy, with suitable compositions x_S and x_B , the band edge effective mass potential are uniquely related to each other, i.e. $m_{S,B} = m_{S,B}(x_{S,B})$ and $U_{S,B} = U_{S,B}(x_{S,B})$. Therefore, the functions $F(E)$ and $\Phi(E)$ (given by Eqs. (11) and (14)) are nonlinear functions of four independent parameters, say the widths c_W and c_S , and the potentials U_B and U_S . Within the class of step asymmetric QWs, all possible shapes (i.e. the values of the four parameters) that provide resonance conditions are accessed by solving the system of three nonlinear equations which demand that the two bound and the continuum resonance state are spaced by exactly $\hbar\omega$:

$$\Phi(U_B, U_S, c_W, c_S, E_0) = 0,$$

$$\Phi(U_B, U_S, c_W, c_S, E_0 + \hbar\omega) = 0,$$

$$E_{\text{res}}(U_B, U_S, c_W, c_S) - (E_0 + 2\hbar\omega) = 0, \quad (15)$$

where E_{res} is the first continuum resonance energy, found as position of the first minimum of the function $F(U_B, U_S, c_W, c_S, E)$ given by Eq. (11).

These equations contain the QW structure parameters, and also the ground state energy E_0 , with its value alone being irrelevant for the process we consider, so it is also taken as a parameter on equal footing with layer widths (c_W, c_S) and potentials (U_S, U_B). With a total of five parameters and three equations (15), two of them are really free “QW design” input parameters, while the remaining three can be determined by solving Eq. (15). Therefore, not only that a QW may be designed for a chosen $\hbar\omega$ (within some limits), but there is even room for the QW shape optimization in order to give maximal nonlinearity. The optimal QW shape may be found by defining a two-dimensional parameter space, to be searched by first solving Eq. (15) for the remaining parameters, and then (provided that the solution is physically and technologically acceptable) calculating the matrix elements and the nonlinear susceptibility corresponding to a particular solution.

Similarly, the described procedure may be employed for optimization of (also frequently encountered) coupled QWs in respect to $\chi^{(2)}$. The described procedure is systematic in the sense that it allows the entire search of the free-parameters space defining the

QW profile within a given class (i.e. of the same general shape), and does not include intuition or elements of luck in spotting the “best potential shape”.

3. Numerical results

The theory described in the previous section was employed for the design and optimization of step asymmetric QWs based on $\text{Al}_x\text{Ga}_{1-x}\text{As}$ alloy, to be used for resonant second harmonic generation of $\hbar\omega = 240$ meV radiation (this corresponds to $5.1 \mu\text{m}$ CO laser or approximately to frequency doubled CO_2 used as pump for the next SHG). The procedure was then repeated for pump photon energy in the range $\hbar\omega = 200\text{--}300$ meV. Due to comparatively large photon energies involved, technologically favorable $\text{Al}_x\text{Ga}_{1-x}\text{As}$ alloy does not provide sufficient band offset for classical three bound-states resonant SHG, and the problem was circumvented by introducing bound–continuum transitions.

In a step QW as displayed in Fig. 1, made of GaAs and AlAs compounds, i.e. with the structure $\text{Al}_{x_1}\text{Ga}_{1-x_1}\text{As}/\text{GaAs}/\text{Al}_{x_2}\text{Ga}_{1-x_2}\text{As}/\text{Al}_{x_1}\text{Ga}_{1-x_1}\text{As}$, the effective mass in separate layers is given by

$$m_B = [m_{\text{AlAs}}x_1 + m_{\text{GaAs}}(1 - x_1)] \left[1 + \frac{E - U_B}{E_{gB}} \right],$$

$$m_S = [m_{\text{AlAs}}x_2 + m_{\text{GaAs}}(1 - x_2)] \left[1 + \frac{E - U_S}{E_{gS}} \right],$$

$$m_W = m_{\text{GaAs}} \left[1 + \frac{E}{E_{gW}} \right] \quad (16)$$

as follows from Vegard’s law and the way chosen to introduce nonparabolicity, with band gaps in the step and barrier layers $E_{gB} = E_{g\text{AlAs}}x_1 + E_{g\text{GaAs}}(1 - x_1)$ and $E_{gS} = E_{g\text{AlAs}}x_2 + E_{g\text{GaAs}}(1 - x_2)$. The barrier and step heights are $U_{B,S} = x_{1,2}\Delta E_c$, where ΔE_c is the conduction band offset between AlAs and GaAs compounds. The nonlinear susceptibility $\chi^{(2)}$ is directly related to the parameter Π^* , Eq. (4), which, upon changing the integration over k_B to integration over $E = E_{k_B}$, and using Eq. (16), reads

$$\Pi^* = M_{01} \sqrt{\frac{2m_{B0}}{\hbar^2}} \frac{1}{\pi}$$

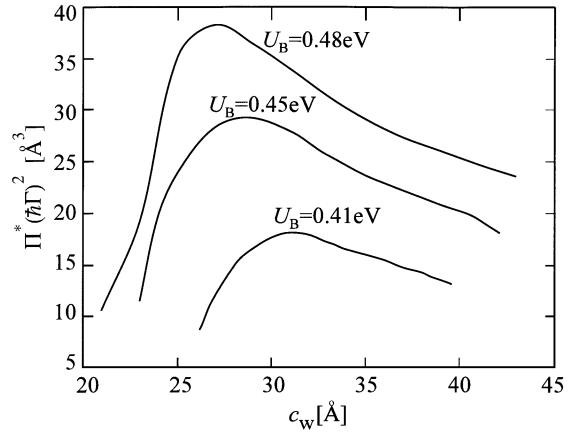


Fig. 2. The optimized values of the matrix elements product $\Pi^*(\hbar\Gamma)^2$, Eq. (17), obtained with different choices of U_B and c_W at $\hbar\omega = 240$ meV.

$$\times \int_{U_B}^{+\infty} \frac{\hat{M}_{0k_B} \hat{M}_{1k_B}}{(\hbar\Gamma)^2 + [2\hbar\omega - (E_{k_B} - E_0)]^2}$$

$$\times \left(\frac{1}{2\sqrt{E_{k_B} - U_B}} + \frac{1}{\sqrt{E_{gB}}} \right) dE_{k_B}, \quad (17)$$

where $m_{B0} = m_{\text{AlAs}}x_1 + m_{\text{GaAs}}(1 - x_1)$ is the conduction band edge effective mass in the barrier.

The material parameters are taken as [24]: $m_{\text{GaAs}} = 0.067m_0$, $m_{\text{AlAs}} = 0.15m_0$, (m_0 -free electron mass), $E_{g\text{GaAs}} = 1.42$ eV, $E_{g\text{AlAs}} = 2.67$ eV, $\Delta E_c = 750$ meV, and $\hbar\Gamma = 5$ meV. In the first set of calculations, we performed the step QW optimization, via solving system (15), by taking the well width c_W and barrier height U_B as free parameters. Other parameters (c_S, U_S, E_0) where coming out from the solution of Eq. (15). In Fig. 2, we give the optimized parameter Π^* as it depends on c_W and U_B (for convenience, Π^* is multiplied with $(\hbar\Gamma)^2$ to become dimensionally equivalent to the product of matrix elements with all three bound states, i.e. $[\text{Å}^3]$). To obtain as large nonlinearity as possible, it is clearly advantageous to choose the highest technologically reasonable barrier height, and, upon fixing this value, there is an optimal well width. Similarly, in Fig. 3, the dependence of $\Pi^*(\hbar\Gamma)^2$ on U_B and the step layer width c_S is

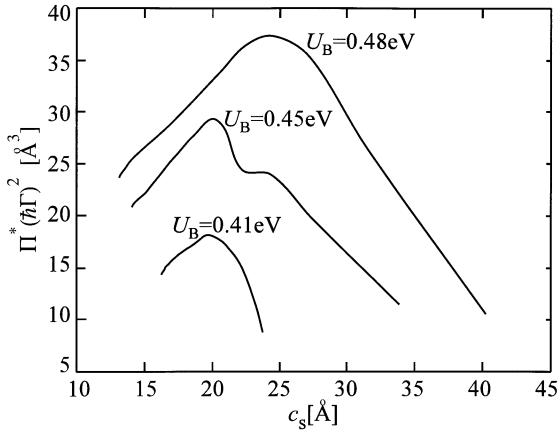


Fig. 3. Same as Fig. 2, but with different choices of U_B and c_S .

given. The largest value $[\Pi^*(\hbar\Gamma)^2]_{\text{MAX}} = 38 \text{ \AA}^3$ is obtained in QW with $U_B = 480 \text{ meV}$, $U_S = 190 \text{ meV}$, $c_W = 27 \text{ \AA}$ and $c_S = 24.5 \text{ \AA}$.

It is not straightforward to compare this result against those obtained in QWs with all three bound states, because few calculations for this pump photon energy have been done so far. In Ref. [29] such a QW was designed, based on nitride semiconductor AlGaIn, and largest value of the matrix elements product amounted to $\Pi \approx 240 \text{ \AA}^3$. The resonant susceptibility $\chi^{(2)} \sim \Pi/(\hbar\Gamma)^2$ would be six times larger than obtained in this work, but only if the linewidths for all three transitions in AlGaIn well is really $\hbar\Gamma = 5 \text{ meV}$. In reality, however, larger linewidths should be expected for transitions to higher levels, as mentioned above, which will proportionally decrease $\chi^{(2)}$ in AlGaIn QW, and will only marginally affect $\chi^{(2)}$ in the QW considered in this paper. Therefore, we expect the susceptibilities in the two structures to become roughly comparable, and one advantage of using resonant state in AlGaAs QW is in the fact that AlGaAs is much better understood technologically than AlGaIn.

The procedure was then repeated for various values of pump photon energy in the range $\hbar\omega = 200\text{--}300 \text{ meV}$. The fully optimized values $[\Pi^*(\hbar\Gamma)^2]_{\text{MAX}}$ and corresponding optimal QW parameters, as they depend on $\hbar\omega$, are presented in Fig. 4. One may note that $[\Pi^*(\hbar\Gamma)^2]_{\text{MAX}}$ decreases with $\hbar\omega$, which is in qualitative agreement with the fact that simple idealized structures, like constant mass linear har-

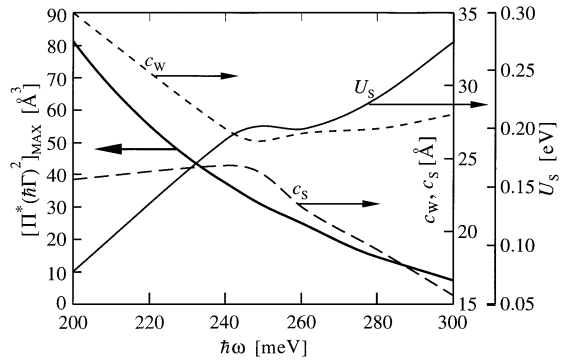


Fig. 4. The fully optimized values of $\Pi^*(\hbar\Gamma)^2$ obtainable at various pump photon energies.

monic oscillator, have dipole matrix elements scaling as $(\hbar\omega)^{-1/2}$, hence one normally expects that $[\Pi^*(\hbar\Gamma)^2] \sim (\hbar\omega)^{-3/2}$ [14].

4. Conclusion

A systematic method for the optimization of ternary semiconductor alloys-based QWs in respect to higher-energy nonlinear optical susceptibility which relies on bound–continuum transitions, was discussed. The method is applicable to step graded QWs, like asymmetric step QWs, coupled QWs and similar, and relies on finding the solution to the system of nonlinear equations. Even though the values of the dipole matrix elements product in semiconductor QW with equispaced two bound states and a continuum resonance state are not very large, it is important to know that it is possible to obtain resonantly enhanced nonlinear optical susceptibility, corresponding to higher values of pump photon energies, in conventional technologically favorable $\text{Al}_x\text{Ga}_{1-x}\text{As}$ based QWs. Maximizing its value via the optimization procedure described may make the effect potentially useful at wavelengths which suitable QWs with three bound states cannot be designed. Similarly, QWs intended for other nonlinear processes which may not require equispaced states (off-resonant harmonic generation, parametric down conversion, etc.) can be optimized in the same fashion, as well.

Appendix

The scattering states Ψ_L and Ψ_R (7)–(8) are orthogonal, and complex-valued functions. These two may be transformed into also orthogonal, but real functions by a suitable unitary transform. The most general form of a 2×2 unitary matrix is

$$\hat{U} = \begin{bmatrix} \cos \alpha e^{i\delta} & \sin \alpha e^{i(\beta+\delta)} \\ \sin \alpha e^{i\gamma} & -\cos \alpha e^{i(\beta+\gamma)} \end{bmatrix}, \quad (\text{A.1})$$

where α , β , γ and δ are arbitrary real parameters. Out of these four, only α and β have nontrivial effect, while γ and δ constitute just a global phase of the two states resulting from application of \hat{U} to Ψ_L and Ψ_R (hence one can immediately set $\gamma = \delta = 0$).

We now require the states Ψ_1 and Ψ_2

$$\begin{bmatrix} \Psi_1 \\ \Psi_2 \end{bmatrix} = \hat{U} \begin{bmatrix} \Psi_R \\ \Psi_L \end{bmatrix} \quad (\text{A.2})$$

to be currentless, which is equivalent to their wave functions being real, i.e. $\text{Im}\{\Psi_{1,2} d\Psi_{1,2}^*/dz - \Psi_{1,2}^* d\Psi_{1,2}/dz\} = 0$. Imposing these conditions on both the right- and left-hand side delivers in four equations, which are, however, all equivalent if we recall that $T_L = T_R \equiv T$, $|T|^2 + |R_{L,R}|^2 = 1$ and $R_L/T = -R_R^*/T^*$ [30], so there is a single condition to be satisfied by two parameters α and β :

$$\cos(2\alpha) + \sin(2\alpha)a \cos(\varphi + \beta) = 0, \quad (\text{A.3})$$

where $R_L/T \equiv ae^{i\varphi}$. There is, therefore, no unique solution, and one may set, e.g. $\alpha = \pi/4$, wherefrom $\beta = \pi/2 - \varphi$ and using $R_L/R_R = -e^{i2\varphi}$, we immediately find that the two real and orthogonal states are given by Eqs. (12) and (13) in the main text.

Using the parameterized representation of the transmission and reflection coefficients [30]: $T = \cos \theta e^{i\tau}$, $R_L = i \sin \theta e^{(\tau+\rho)}$ and $R_R = i \sin \theta e^{(\tau-\rho)}$ where θ , τ and ρ are real, the asymptotic expressions for Ψ_1 and Ψ_2 , up to a constant phase factor, read

$$\begin{aligned} \Psi_1(z \rightarrow \pm\infty) &= \cos\left(k_z z + \frac{\pm\theta \pm \tau - \rho}{2}\right), \\ \Psi_2(z \rightarrow \pm\infty) &= \sin\left(k_z z - \frac{\rho \pm \theta \pm \tau}{2}\right). \end{aligned} \quad (\text{A.4})$$

References

- [1] F. Capasso, MRS Bull. 16 (1991) 23.
- [2] E. Rosencher, A. Fiore, B. Vinter, V. Berger, Ph Bois, J. Nagle, Science 271 (1996) 168.
- [3] E. Rosencher, Ph. Bois, J. Nagle, S. Delaitre, Electr. Lett. 25 (1989) 1063.
- [4] P. Boucaud, F.H. Julien, D.D. Yang, J.M. Lourtiouz, E. Rosencher, Ph. Bois, J. Nagle, Appl. Phys. Lett. 57 (1990) 215.
- [5] E. Rosencher, Ph. Bois, Phys. Rev. B 44 (1991) 11 315.
- [6] Ph. Bois, E. Rosencher, J. Nagle, E. Martinet, P. Boucaud, F.H. Juleien, D.D. Yang, J. M. Lourtiouz, Superlatt. Microstr. 8 (1990) 369.
- [7] S.J.B. Yoo, M.M. Fejer, R.L. Byer, Appl. Phys. Lett. 58 (1991) 1724.
- [8] M.M. Fejer, S.J.B. Yoo, R.L. Byer, J.S. Harris Jr., Phys. Rev. Lett. 62 (1989) 1041.
- [9] Z. Ikonić, V. Milanović, D. Tjapkin, IEEE J. Quantum Electron. 25 (1989) 54.
- [10] C. Sirtori, F. Capasso, D.L. Sivco, A.L. Hutchinson, A.Y. Cho, Appl. Phys. Lett. 60 (1992) 151.
- [11] F. Capasso, C. Sirtori, A.Y. Cho, IEEE J. Quantum Electron. 30 (1994) 1313.
- [12] C. Lien, Y. Huang, T.-F. Lei, J. Appl. Phys. 75 (1994) 2177.
- [13] V. Milanović, Z. Ikonić, IEEE J. Quantum Electron. 32 (1996) 1316.
- [14] V. Milanović, Z. Ikonić, D. Indjin, Phys. Rev. B 53 (1996) 10887.
- [15] V. Milanović, Z. Ikonić, J. Appl. Phys. 81 (1997) 6479.
- [16] V. Milanović, Z. Ikonić, Solid State Commun. 104 (1997) 445.
- [17] J.N. Heyman, K. Craig, M. Sherwin, K. Campan, P.F. Hopkins, S. Fafard, A.C. Gossard, in: H.C. Liu et al. (Eds.), Quantum Well Intersubband Transition Physics and Devices, Kluwer Academic Publishers, Dordrecht, 1994, pp. 467–476.
- [18] Z. Ikonić, V. Milanović, D. Tjapkin, Appl. Phys. Lett. 54 (1989) 247.
- [19] S.J. Li, J.B. Khurgin, J. Appl. Phys. 73 (1993) 4367.
- [20] Rusli, T.C. Chong, S.J. Chua, Jpn. J. Appl. Phys. 32 (1993) 1998.
- [21] L.C. Lenchyshyn, H.C. Liu, M. Buchanan, Z.R. Wasilewski, J. Appl. Phys. 79 (1996) 3307.
- [22] T. Mei, G. Karunasiri, S.J. Chua, Appl. Phys. Lett. 71 (1997) 2017.
- [23] M. Bendantay, R. Kapon, R. Beserman, A. Sa'ar, R. Planel, Phys. Rev. B 56 (1997) 9239.
- [24] G. Bastard, Wave Mechanics Applied to Semiconductor-Heterostructure, Les Editions de Physique, Les Ulis, France, 1990.
- [25] D.F. Nelson, R.C. Miller, D.A. Kleinman, Phys. Rev. B 35 (1987) 7770.
- [26] M.G. Rozman, P. Reinker, R. Tehrer, Phys. Rev. A 49 (1994) 3310.

- [27] T. Mizuno, M. Eto, K. Kawamura, *J. Phys. Soc. Japan* 63 (1994) 2658.
- [28] D. Dragoman, M. Dragoman, *IEEE J. Quantum Electron.* 32 (1996) 1150.
- [29] D. Indjin, Z. Ikonić, V. Milanović, J. Radovanović, *IEEE J. Quantum Electron.* 34 (1998) 795.
- [30] G. Barton, *J. Phys. A* 18 (1985) 779.